ENHANCED THERMAL BEHAVIOR, MECHANICAL PROPERTIES AND UV SHIELDING OF POLYLACTIC ACID (PLA) COMPOSITES REINFORCED WITH NANOCRYSTALLINE CELLULOSE AND FILLED WITH NANOSERICITE

CHIH-PING CHANG, I-CHEN WANG,* YUAN-SHING PERNG**

National Chung Hsing University, Department of Forestry, 40227, Taichung, Taiwan
**Taiwan Forestry Research Institute, Division of Wood Cellulose, 10066, Taipei, Taiwan*
***Da Yeh University, Department of Environmental Engineering, 51591, Changhua, Taiwan*

Received September 3, 2011

The objectives of this study were to utilize nanocrystalline cellulose (NCC) and nanosericite (NS) as reinforcing and functional filling agents compounded in a polylactic acid (PLA) substrate for forming novel nanocomposite materials, and subjecting the composites to field-emission electron microscopy (FE-SEM), tensile strength, thermomechanical analyses, thermal gravimetric analysis and UV-Vis spectroscopic analyses; so as to investigate the effect of the modifications achieved by incorporating the nanomaterials on the surface properties, tensile strength, glass transition temperature (T_g), storage modulus, thermal gravimetric loss and shielding efficacy against UV light of different wavelengths. The results indicated that adding suitable quantities of NS and/or NCC to a PLA substrate could improve the overall thermal stability, mechanical strength and UV shielding capacity of the resulting nanocomposites. The shortcoming of weak bonding between NS and PLA could be ameliorated with the addition of NCC. The simultaneous addition of NS and NCC to the composite substrate exerted a greater contribution to the enhancement of the overall functionalities, compared to either bipartite compounds. Based on our results, at a 3% NS and 7% NCC addition rate to the PLA substrate, the most optimal tensile strength was obtained. At temperatures <250 °C, the nanocomposites exhibited good thermal stability and could effectively block about 65% of UVB and UVC irradiation. In the future, the formulations might be applied as a biodegradable UV shielding coating film, or alone, as a medical wrapping material or packaging material.

Keywords: polylactic acid, nanocrystalline cellulose, nanosericite, thermal gravimetric analysis, UV shielding

INTRODUCTION

The main thrust of the 21st century macromolecular R&D has shifted from the traditional petrochemical-based products to green eco-efficient materials that have low consumption of resources and energy, being environmentally friendly and highly renewable, recyclable, as well as biodegradable. Among these, polylactic acid (PLA) is a well-known biodegradable material derived from lactic acid monomers fermented from plant starch and synthesized via various routes to produce polymers of different molecular weights. PLA is a non-toxic and non-stimulant macromolecular material with good biocompatibility, which has been widely applied in medical, industrial, food and agricultural domains.

However, typical PLA is a linear polymer often with poor cross-links and poorer mechanical strengths, compared to other types of plastics. It is relatively expensive, brittle, with low thermal deformation temperature and no resistance to impact. Therefore, its applications are limited.[1] Many researchers tried incorporating functional reinforcements and fillers to PLA to ameliorate the aforementioned shortcomings. These functional ingredients often include inorganic minerals, minute metal particles and organic or inorganic fibrous polymers.

Previous research has suggested that adding inorganic minerals to PLA could enhance the overall thermal stability, impact resistance, UV

light shielding effect and electrical conductivity etc. Widely used inorganic minerals include titanium dioxide, montmorillonite, bentonite, layered silicates, and mica.[2-5] Prior studies also indicate that adding inorganic minerals at a <10% ratio could significantly improve all the shortcomings of PLA. However, at addition rates >10%, the stacking of the mineral particles in the composites would cause loss of mechanical strengths.[6,7] In this study, we attempted the application of sericite, an endemic mica mineral produced in the Taitung area of Taiwan, which is present in ample quantities, has a good production rate and reasonable pricing. Exfoliating the stacked platy layered mineral into a nanoscale preparation would allow its incorporation into a macromolecular polymer substrate as functional filler.

Besides the addition of inorganic materials to polymer substrates, in recent years, the technologies of utilizing biological fibrous materials as functional additives for reinforcing composite networks have also come of age. In particular, the applications of cellulosic preparations have received most attention. Cellulose is a biopolymer that exists in nature in great quantities. It is a renewable and biodegradable material. The long-chain molecules of cellulose have regular crystalline regions and superior mechanical strengths. However, direct deployment of plant fibers or micrometer scale microcrystalline cellulose (MCC) can not achieve homogeneous blending with the polymer substrate, nor improve oxygen permeation and tensile modulus of the composite, but only marginally enhance the yielding strength of the polymer. On the other hand, if macroscopic cellulose is reduced to nanometer scale nanocrystalline cellulose (NCC), the vastly increased specific surface area of the NCC then ensures effective increases of bonding between NCC and polymer substrate. Other advantages of using NCC as a functional additive include a safe return to ambient carbon cycle, very high Young's modulus and tensile strength, roughly 25% of those of nanocarbon tubes, greatly expanded specific surface area, high surface energy and chemical activity, thus effectively moderating the optical, thermal, electrical, insulational, or even superconductivity properties of the composites incorporating them. By adjusting the amount of NCC, the resulting products could possess good light transparency, strengths, surface properties, thermal properties and biodegradability.[6,8-12]

There have been reported numerous studies examining the properties of composite materials incorporating a single functional additive.[13-17] There are, however, scanty reports on multiple-component nanocomposites. Therefore, we endeavored to transform native sericite and cotton linter into nanoscale functional products and incorporate them into a PLA substrate to produce a series of bi- and tripartite nanocomposites in a bid to rectify many shortcomings of traditional PLA products and examine the novel functionalities exhibited by the resulting nanocomposites.

EXPERIMENTAL

Design

This study aimed at preparing nanocomposites by compounding NCC and NS with the L-type PLA, and analyze the mechanical and thermomechanical properties, and the UV shielding capacity of the resulting products. Furthermore, the interactions between NS and MCC with PLC, and between NS and NCC were examined with a view to providing suitable explanations to the changes in composite properties.

The NS and NCC were individually compounded with PLA at wt/wt dosage ratios of 1, 3, 5, 7 and 9% to form films, and then determine their properties. Subsequently, using the tensile strength performance as a culling factor, we used the 3% NS dosage as the optimal, and at a fixed NS dosage, 1, 3, 5, 7 and 9% of NCC were then added to the PLA substrate to form nanocomposite films. The film properties were then determined. In order to comprehend the various properties of the resulting nanocomposites, we subjected the film specimens to tensile tests, field-emission scanning electron microscopy (FE-SEM), thermal gravimetric analysis (TGA), dynamic mechanical analysis (DMA), and UV-Vis spectroscopic analysis. Thus, the mechanical strengths, external morphology, thermal gravimetric properties, glass transition temperatures (T_g) and UV shielding capacity of the nanocomposites were determined.

Materials

The NCC used in this study was produced in the laboratory by sulfuric acid hydrolysis of cotton linter. The materials used in the study, including cotton linter and chemicals were as follows: Sericite 080715 (Sunshine Mineral Co. Ltd., Taitung, Taiwan), cotton linter (Chung-Rhy Specialty Paper Co., Puli, Taiwan), phosphoric acid, 98% sulfuric acid and sodium hydroxide (AR, Panreac Quimica S.A.U., Spain), tetrahydrofuran or THF (AR, Acros, U.S.A.), and poly-L-lactic acid with molecular weight of 180,000~200,000 (reagent grade, Wei Mon Industry Co. ltd., Taipei, Taiwan). In the study, the

self-prepared NS was of a platy structure, with length and width of ca. 300 nm and thickness of 40 nm, with a specific surface area of ca. 200 to 350 $m^2 g^{-1}$, a pH of 7.5±1, and a cationic exchange capacity (CEC) of 0.859 meq g^{-1}. The NCC preparation had an aspect ratio of 34.0, with modal length between 150 to 500 nm and crystallinity of 85.5.[18]

Analytical instruments

A coating applicator (ZFR2403, Zehntner, Switzerland) was used to prepare the PLA nanocomposite films. The surfaces of the nanocomposites and the mixing conditions of the functional additives with the PLA polymer substrate were observed with an FE-SEM (JSM7401F, Jeol Inc., Tokyo, Japan). In order to comprehend the mechanical strength of the nanocomposites, an EZ-Test, Shimadzu Co., Tokyo, Japan) was used for the tensile test of the polymer films. The thermomechanical and thermal gravimetric degradation properties of the nanocomposites were determined, respectively, with a dynamic mechanical analyzer (DMA8000, PerkinElmer, Waltham, MA, USA) and a thermal gravimetric analysis unit (Pyris 1, PerkinElmer, Waltham, MA, USA). The shielding capacities against UVA, UVB and UVC were measured using a UV-Vis spectroscopy (HP8452, Agilent Technologies Inc. Santa Clara, CA, USA).

Methods

The NCC was prepared in the laboratory using sulfuric acid hydrolysis of cotton linter. The conditions of hydrolysis employed were the following: acid concentration of 55%, solid to liquor ratio of 1:15, reaction temperature of 50 °C, and reaction time of 10 min. The NS was also prepared in the lab, first by using a 40% NaOH solution to exchange the inter-layer potassium ion, achieving intercalation of sodium ion. Then phosphoric acid was added to the intercalated sericite to swell the mineral and diminish it to an exfoliated nano-dimensional state with a translucent gel-like appearance. Subsequently, the pH of the gel was adjusted to neutrality and the acid was removed by dialysis. Then the NS preparation was oven-dried and stored.

The procedure for the preparation of PLA nanocomposites entailed the following: the PLA pellets were dissolved in THF at a solid to liquid ratio of 1:20, the NS and NCC were accurately weighed based on the mass of PLA, and the materials were stirred with a magnetic stirrer for 24 h for compounding. The PLA liquor was subjected to 20 min of ultrasonic oscillation in an ultrasonic bath to degas minute air bubbles before forming into films. Then the coat applicator spread the mother liquor onto a clean glass pane with a gauge setting of 150 μm and 3 coats were applied to each film. The wet films were placed in a hood for 72 h to allow total evaporation of the solvent. An oriented film with an average thickness of 300 μm was thus obtained. Based on the dosages of the functional additives, we designated the blank PLA film as PLA, the ones with 1, 3, 5, 7 and 9% NS as PS1, PS3, PS5 and so forth; those with added NCC of corresponding proportions, PC1, PC3 and so forth. And finally, after establishing an optimal dosage of NS, the tripartite composites with 1, 3, 5, 7 and 9% of NCC were designated as PS3C1, PS3C3 and so forth.

The samples subjected to the FE-SEM observation were first sputter-coated with platinum, then observed under an electron beam strength of 2 kV. We observed both the original film surfaces and the failed surface after the tensile elongation. The procedure for the tensile test was to first prepare I-shaped test specimens with long edges parallel to the direction of coating with a cutting mold, in accordance with ASTM D638. The length, width and thickness of the tested parts were measured with a micrometer caliper, and the test specimens were stretched to failure using a constant rate of elongation of 5 mm min^{-1}. The stress-strain curve was recorded and the tensile strength and rate of elongation at the point of failure were calculated. Thermomechanical and thermal degradation properties of the nanocomposites were determined using DMA and TGA instruments, respectively. The test specimens for DMA had dimensions of 10 x 7 mm and nominal thickness of 300 nm. The test was conducted under a tensile mode and the samples were scanned using a fixed frequency of the temperature rise mode. The frequency was 1 Hz s^{-1}, the temperature range of 30~180 °C, and the temperature rise rate of 5 °C min^{-1}. The T_g and storage modulus of the nanocomposites were recorded by the instrument. The thermal degradation behavior of the PLA nanocomposites were determined using a 10 °C min^{-1} rise rate, and a temperature range from 50 to 400 °C in a TGA unit. An atmosphere of nitrogen was applied with a gas flow rate of 20 mL min^{-1}. The procedure for determining the UVB and UVC shielding capacity was to subject a 10% solids content THF blank PLA mother liquor, as well as suspensions of NS and NCC in THF individually, to a UV-Vis scanning from 200 to 400 nm wavelength for UV attenuation. Films of the nanocomposites were cut into long strips of 50 x 7 mm, clamped securely with a pair of clamps and then tested for UV attenuation. The experiments were replicated 5 times.

RESULTS AND DISCUSSION

We compounded NS and NCC with PLA and prepared films of nanocomposites. Through the control of inorganic dosage, the overall mechanical strengths of the composite could be enhanced. The good barrier property afforded by the platy structure of the NS inorganic material could endow good UV shielding capacity to the resulting composite; whereas the elongated NCC could potentially endow the composite with

elasticity and mechanical reinforcement. Based on the experimental results, we analyzed the distribution characteristics of the functional additives in the polymer substrate and their effects on the overall tensile strength, as well as the various thermal and UV shielding properties of the nanocomposites.

Distribution of functional additives in the polymer substrate

The external appearances of the nanocomposites are shown in Fig. 1. The results indicate that adding large quantities of NS and NCC caused the composites to become opaque. Comparing Fig. 1b with 1f, and 1g with 1k, it is discernible that NS affected the transparency of the composites to a greater degree than NCC. The FE-SEM observational results are shown in Fig. 2. From Fig. 2a, it can be discerned that when no functional additive was added, the surface of the PLA film was rough and uneven and rife with minute holes caused by the evaporation of solvent.

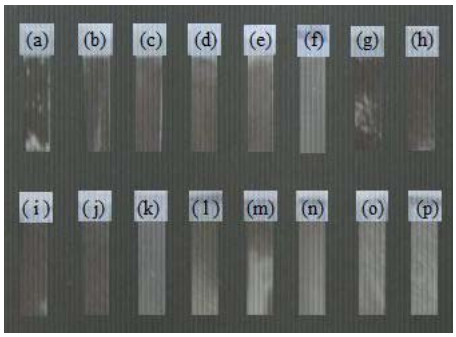

Figure 1: Appearances of prepared nanocomposites (a) PLA; (b) PS1; (c) PS3; (d) PS5; (e) PS7; (f) PS9; (g) PC1; (h) PC3; (i) PC5; (j) PC7; (k) PC9; (l) PS3C1; (m) PS3C3; (n) PS3C5; (o) PS3C7; and (p) PS3C9

Compared to Fig. 2b, when stretched by an external force, the holes on the PLA film surface became more prominent, causing the film to lose integrity and mechanical strength. Fig. 2c shows the FE-SEM micrograph of PC9 surface, on the left, it shows the normal state of the surface, while the right half shows the distribution of NCCs in the PLA substrate when the surface layer was removed. The figure indicates that incorporating NCC helps the composite surface to remain smooth. Furthermore, NCC distributed evenly in the PLA substrate and formed a network of intersecting segments. Figure 2d shows that when the nanocomposite was subjected to an external force and failed, the NCC also broke in a ladder-like fashion. Also, there appeared to be no distinctive boundaries between NCC and the PLA substrate, indicating that NCC was not merely embedded in the substrate, but rather formed effective reinforcing bonding with the substrate. Figures 2e and 2f suggest that when the NS dosage was less than 5%, NS could distribute evenly in the PLA substrate and tended to fill surface voids of PLA causing the surface to become smoother. If, however, the NS dosage was >7%, then NS protruded and accumulated on the surface of the nanocomposite.

Figure 2f also shows that when subjected to a failure-causing external force, there appeared to be interstices between the seams of NS and PLA, leading to marked strength loss. Figure 2g shows that too much NCC tended to push NS toward the surface of PLA, causing an overall uneven distribution of the nanomaterials. Figure 2h indicates that the addition of NCC could ameliorate the propensity of seam breakage between NC and PLA substrate when subjected to an external force and initiated failure of the composite.

Analysis of mechanical strength performance

The tensile performance of the nanocomposites and the stress-strain graph are shown in Table 1 and Fig. 3. The table shows that adding independently NS and NCC was helpful to enhance the tensile strength of PLA, with the best performance derived from PS3, which increased the tensile strength of PLA from 28.1 MPa to 45.4 MPa. The 3% NS dosage was thus deemed as the optimal for the subsequent tripartite addition dosage. Adding only 1% NS could increase the tensile strength to 39.5 MPa, showing a very high specific interaction. With NS dosages >5%, however, the tensile strength reverted to lower

levels. Thus, adding small quantities of NS was helpful to increase the tensile performance of the nanocomposites, while greater amounts were not effective. The pure PLA film had a rate of elongation at break of 42.8%, but with increasing addition of NS, the rate decreased markedly, rendering the nanocomposites stiffer and brittle.

According to the study of Uno *et al.*,[5] the phenomenon was caused merely by the physical intercalation of PLA with NS, and there was no formation of chemical bonding between them. On the other hand, adding NCC to the PLA substrate alone, at NCC dosages greater than 5%, the rate of elongation at break showed further increases. Compared to Fig. 2c, this phenomenon might be caused by NCC automatically forming intersecting networks.[12,19] Simultaneously adding NS and NCC to PLA gave better overall rates of elongation at break than those obtained when adding NS or NCC alone. Among the tripartite nanocomposites, the PS3C7 exhibited the highest tensile strength, of 49.0 MPa, and a rate of elongation at break of 36.8%.

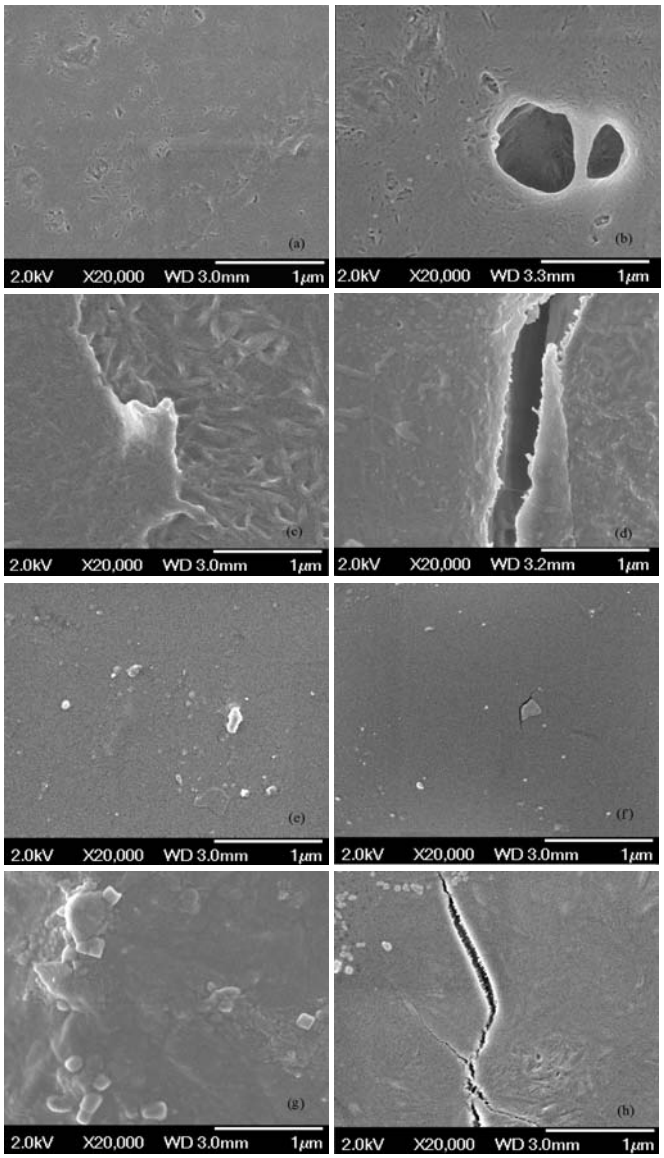

Figure 2: FE-SEM micrographs of the surfaces of nanocomposites (a) PLA; (b) tensile failed PLA film; (c) PC7; (d) tensile failed PC7 film; (e) PS7; (f) tensile failed PS3 film; (g) PS3C7; and (h) tensile failed PS3C7 film

Table 1
Tensile properties of the PLA/NS/NCC nanocomposite films

Sample	Functional filler (%)		Max. tensile strength (Mpa)	Elongation at break (%)
	NS	NCC		
PLA	0	0	28.1	42.8
PS	1	0	43.4	31.8
	3		45.4	22.6
	5		21.4	22.2
	7		27.1	25.1
	9		22.7	16.0
PC	0	1	33.5	25.4
		3	32.7	18.1
		5	28.2	20.0
		7	33.9	30.4
		9	29.6	27.4
PS3C	3	1	42.2	42.0
		3	32.8	36.6
		5	35.9	34.8
		7	49.0	36.8
		9	33.7	22.8

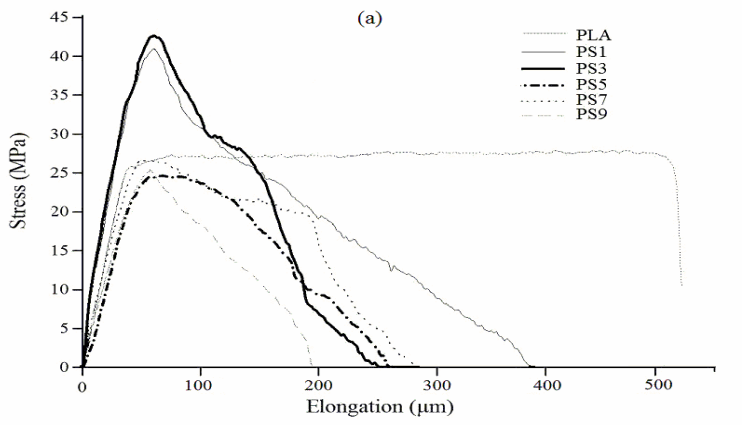

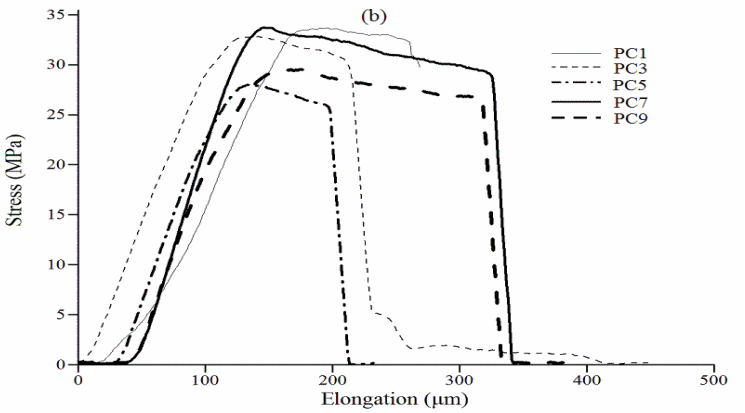

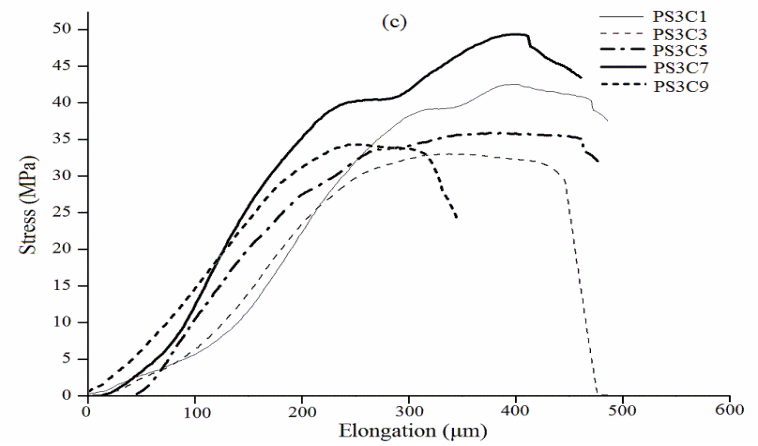

Figure 3: Stress-strain curves of nanocomposites (a) PLA and PS1~9; (b) PC1~9; and (c) PS3C1~9

Table 2
Thermal degradation parameters measured by TGA analyses for PLA/NS/NCC nanocomposites

Sample	First stage		Second stage		Third stage		TWLR (%)
	Onset temp. (°C)	WLR (%)	Onset temp. (°C)	WLR (%)	Onset temp. (°C)	WLR (%)	
NS	49.4	1.5	203	3.0			4.5
NCC	146.4	10.0	205.2	29.2	258.2	22.5	66.3
PLA	266.6	92.7	-	-	-	-	99.4
PS1	249.9	97.8	-	-	-	-	98.4
PS3	288.6	96.2	-	-	-	-	97.5
PS5	290.3	91.6	-	-	-	-	95.1
PS7	297.6	90.9	-	-	-	-	93.8
PS9	299.8	91.6	-	-	-	-	93.8
PC1	322.3	92.3	-	-	-	-	98.0
PC3	318.5	91.6	-	-	-	-	97.5
PC5	240.8	2.9	330.7	91.1	-	-	96.5
PC7	242.9	19.3	309.6	72.3	-	-	96.5
PC9	238.7	12.2	262.3	8.9	310.7	57.4	95.5
PS3C1	344.1	95.5	-	-	-	-	97.0
PS3C3	241.4	1.3	346.9	91.2	-	-	94.7
PS3C5	257.8	2.0	341.5	92.5	-	-	96.5
PS3C7	247.3	6.2	274.2	11.5	334.5	73.7	94.8
PS3C9	235.8	3.5	326.7	88.2	-	-	94.6

WLR: weight loss rate
TWLR: total weight loss rate

Analyses of thermal properties of the nanocomposites

Figure 4 shows the thermal gravimetric (TGA) weight loss and the differential thermal gravimetric (DTG) curves. Table 2 shows the pertinent parameters of thermal degradation of the nanocomposites. The TGA results indicate that pure PLA had a thermal degradation temperature of 266.6 °C, and only 1 major degradation stage was discerned. The nanocomposite incorporating NS did not show an altered thermal degradation trend, there was still only 1 main degradation stage. If NS dosages >3%, however, the thermal stability of the composite was enhanced, and with increasing amounts, the onset temperature of thermal degradation also increased. Adding NCC to a nanocomposite could also significantly increase the onset temperature of thermal degradation. Adding 1% NCC and 3% NS raised the onset temperature to 322.3 and 318.5 °C,

respectively; while the thermal degradation trend was not affected. However, when the NCC dosages were >5%, the intrinsic NCC thermal degradation tendencies would show up in the composites. In PC5 and PC7, there were 2 main thermal degradation stages, whereas PC9 exhibited 3 thermal degradation stages. Nevertheless, the dominant thermal degradation still remained between 309 and 330 °C. The first stage weight losses of PC5, 7 and 9 were all greater than the amount of NCC added. A possible explanation was that the NCC did not form significant chemical bridging with the PLA substrate, and was merely interspersed in the amorphous regions of the substrate. Therefore, they tended to degrade simultaneously under high temperatures. The similar situation was also seen in the cases of PS3C3 to PS3C9.

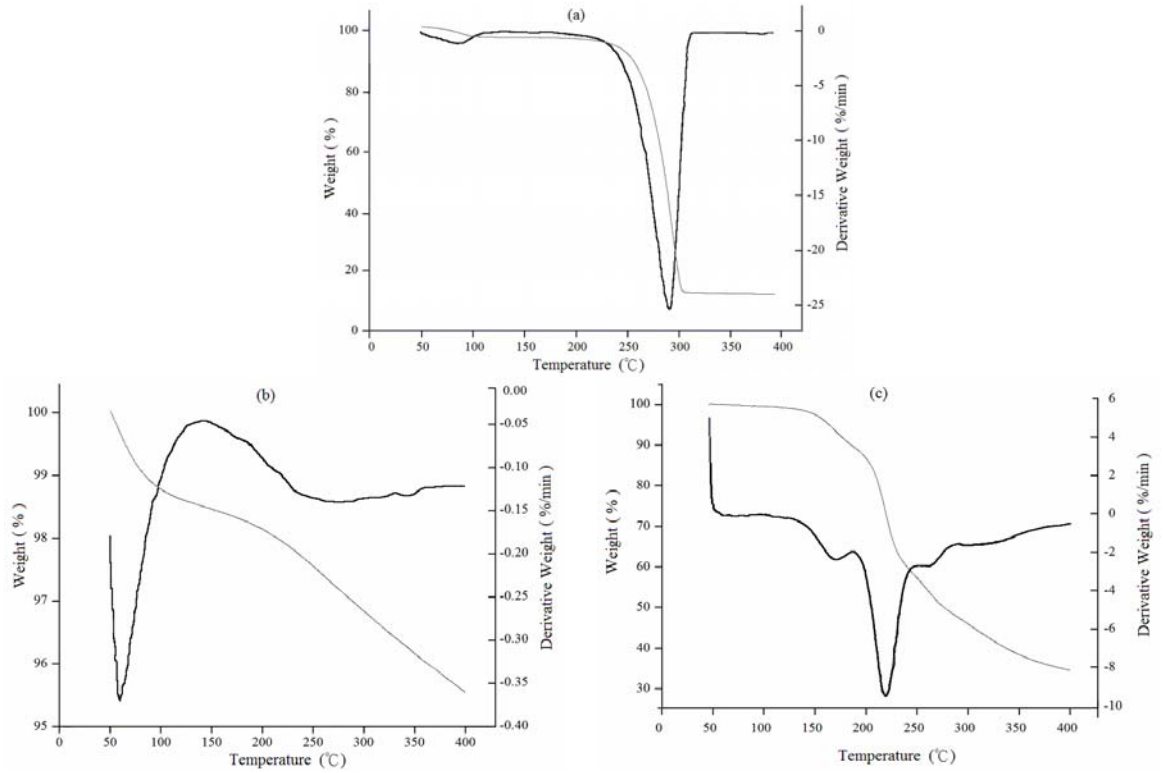

Figure 4: Thermal gravimetric (TG) and DTG curves of nanocomposites (a) PLA; (b) NS; and (c) NCC

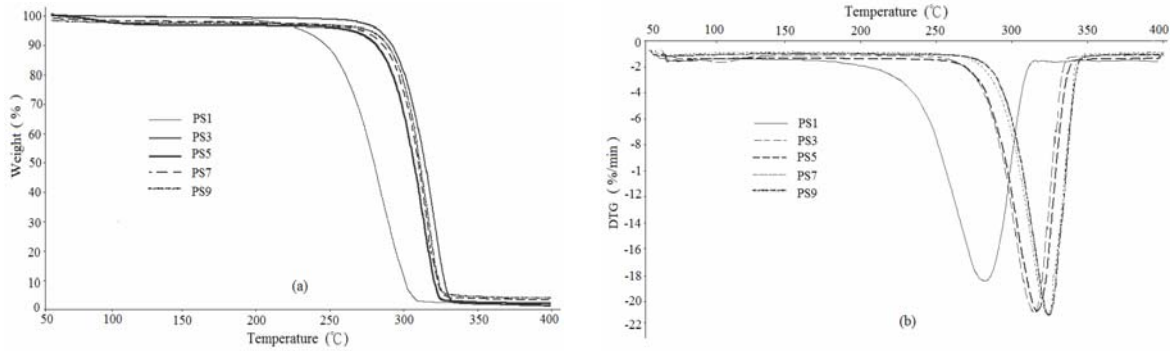

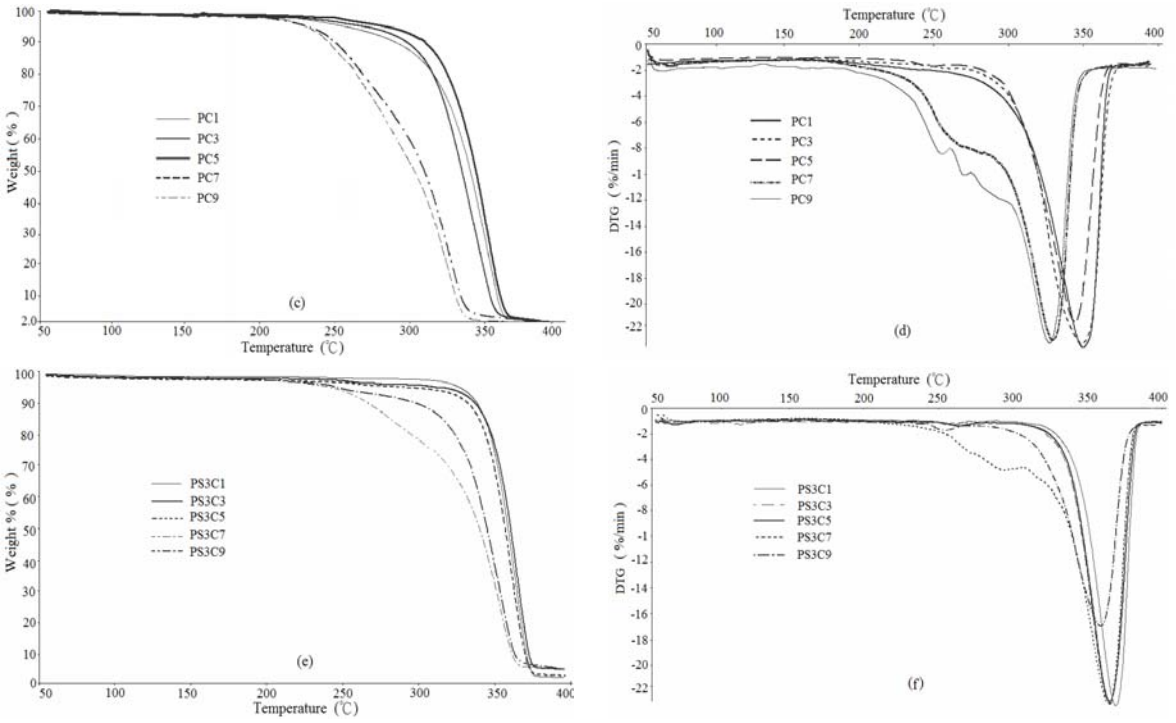

Figure 5: TG and DTG curves of nanocomposites: (a) TG of PS1~9; (b) DTG of PS1~9; (c) TG of PC1~9; (d) DTG of PC1~9; (e) TG of PS3C1~9; and (f) DTG of PS3C1~9

The DMA results and the glass transition (T_g) temperatures of the nanocomposites are shown in Figs. 6. The figures show that pure PLA had a T_g of ca. 75 °C, and according to Henton *et al.*,[1] the bridging structure and degree of crystallinity of PLA could significantly affect its T_g, and that highly crystalline PLA had a T_g between 70 and 80 °C. Figures 6a~6j show that the functional additives tended to decrease the T_g of the composites, as compared to pure PLA. Adding 1% NS caused the T_g to decrease to 55 °C; whereas 1% of NCC decreased the T_g to 60.5 °C, see Fig. 6b and 6d, respectively. Prior studies of other researchers suggest that PLA is a semi-crystalline material, in which the crystalline regions are cross-linked. When subjected to an external force, the crystalline regions maintain the original structure, while the amorphous regions are the main deformation zones. Adding NCC or inorganic substance to the macromolecular polymer would cause PLA to undergo trans-crystallization and form trans-crystals centered around the functional additives, thus altering the thermo-mechanical properties of the composites.[20,21] The DMA results indicate that adding NS could enhance the stiffness of the composite under room temperature conditions. When temperature reached the T_g, however, the overall strength of the composite tended to decrease precipitously. Furthermore, because there was largely no chemical bonding between NS and PLA, and because of the weak intermolecular bonding of the NS molecule layers, the nanocomposites PS1~9 all exhibited total loss of mechanical strength at a temperature of 55~58 °C. Comparing Fig. 6d and 6e and Fig. 2c, NCC in the PLA substrate is thought to form networks that through formations of hydrogen bonding contributed to the integral strength of the composite. Hence, although when heated to the T_g, free volumes of the amorphous regions of the nanocomposites increased, and the storage modulus decreased, still certain strength was retained through the interaction of NCC molecules. Furthermore, when we used lipophilic THF to dissolve PLA and formed a dispersed NCC suspension in it, the surface of NCC was surrounded by THF molecules and there were minuscule interstices between the two entities. When the temperature reached a level higher than the T_g of PLA, the interstices were again filled by the softened PLA, causing PLA to form a more secure physical anchoring with the fibrous NCC, enabling PC1~9 to retain a certain storage module at temperatures above the T_g of these composites. Figures 6f~6j show that when 3% NS together

with NCC at 1~9% were added to the PLA substrate, the nanocomposites often had higher T_g than those with NS or NCC alone. The 3 nanocomposites, PS3C5~C9, showed increases in their storage module after exceeding their T_g points. The probable reason for the phenomenon could be the anchoring interactions between the functional additives and PLA, there might also be interactions between NCC and NS, such as hydrogen bonding between the hydroxyl groups existing on both types of additives. The question as to whether there are chemical bonds and what kinds of bonds they are remains unresolved. Further study to delineate the problem is planned.

Shielding capacities of nanocomposites against UVB and UVC

The respective UV transmittance spectra of PLA, NS and NCC are shown in Fig. 7. The UV transmittance data of the nanocomposites are listed in Table 3. Transmittance rates of the nanocomposites were calculated based on selecting directly the four strongest peaks of their UV-Vis spectra, in which, peaks at 254 and 277 nm wavelengths represented the transmittance of UVC; the 300 nm wavelength represented the transmittance of UVB; and the 400 nm wavelength stood for the transmittance of UVA. The absorbance function employed logarithm and scalar multiplier functions to transform the spectra into absorbance spectra using the following equation:

$$A = -\log_{10}\left(\frac{T}{100}\right) = -\log\left((I_s - I_{sd})/(I_0 - I_{0d})\right)$$

where A is absorbance; T is percentage transmittance; I_0 is the reference intensity measured with the blank; I_{0d} is the dark current measured immediately before the reference; I_s is the intensity measured with the sample; I_{sd} is the dark current measured immediately before the sample. The variances of the spectrum were transformed using the following equation:

$$\mathrm{var}(A) = \left(\frac{1}{T \cdot \ln 10}\right)^2 \mathrm{var}(T)$$

The transmittance spectra were calculated using the transmittance function. The function used exponential, reciprocal, and scalar multiplier functions to transform the absorbance spectra into transmittance spectra using the following equation:

$$T = 100 \cdot 10^{-A}; \quad \mathrm{var}(T) = \left(100 \cdot \ln 10 \cdot 10^{-A}\right)^2 \cdot \mathrm{var}(A)$$

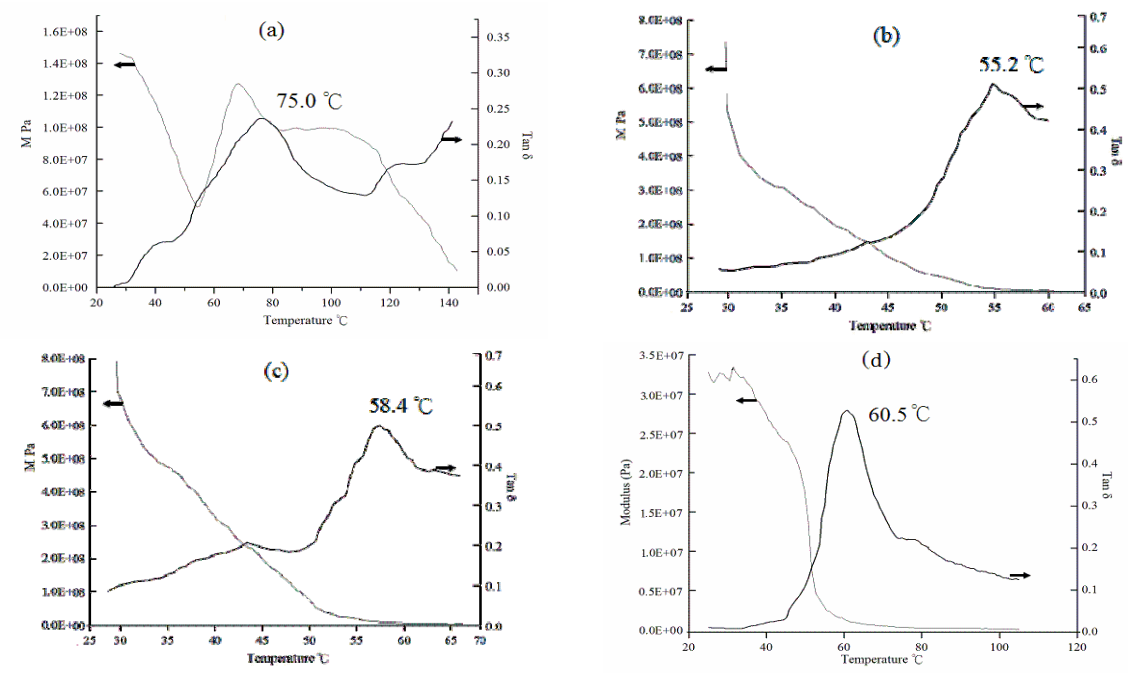

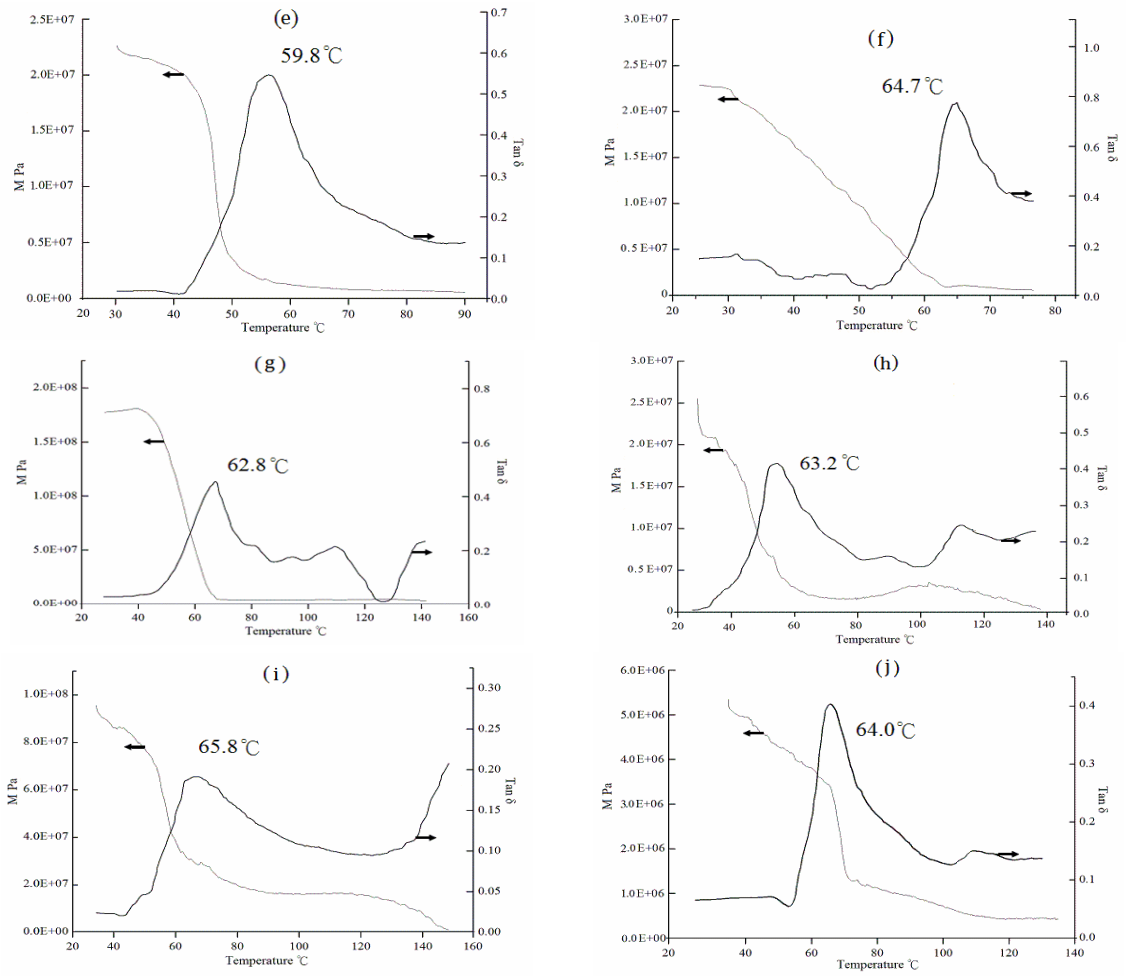

Figure 6: Dynamic mechanical analysis (DMA) thermograms of nanocomposites: (a) PLA; (b) PS1; (c) PS3; (d) PC1; (e) PC7; (f) PS3C1; (g) PS3C3; (h) PS3C5; (i) PS3C7; and (j) PS3C9

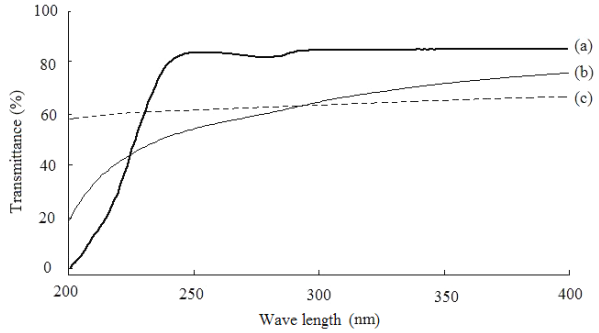

Figure 7: UV transmittance of nanocomposite raw materials (a) PLA; (b) NCC; and (c) NS

According to Fig. 7 and Table 3, pure PLA had nearly no shielding capacity against UV light of wavelength >250 nm; whereas NS possessed certain shielding capacities against UV light of any wavelengths. NCC, on the other hand, had better shielding performances against UVB and UVC. Table 3 indicates that compared to pure PLA, when the NS dosage alone in the composite

reached 5%, it was capable of presenting barriers to block UVB and UVC. The transmittance of UVC at 254 nm decreased 66.2%; at 277 nm decreased 65.1%. The same composite reduced UVB transmittance at 300 nm by 59.5%. The results for PS7 and PS9, however, probably because of the ensuing non-uniform distribution of NS as the self-aggregation of NS produced floc-like patches, these nanocomposites had a spotty resistance to the transmission of UV light, with the film parts containing less NS to have poorer shielding capabilities. Adding NCC alone to the composites provided less effective UV light shielding than when adding NS alone. If both additives were added, however, then the transmittance of UV light could be markedly reduced. For instance, the PS3C7 reduced UVC at 254 nm wavelength by 67.5%; at 277 nm wavelength by 69.1%. Its transmittance of UVB at 300 nm wavelength was also reduced by 64.8%. Even though none of the components showed much shielding efficacy against UVA transmittance alone, upon compounding of the components however, the tripartite composite showed UVA transmittance at 400 nm wavelength by 63.7% lower than that of pure PLA. The transmittances of UVA, UVB and UVC for the PS3C9 preparation showed higher values than those of the PS3C7, however. The probable reason was again due to the uneven distribution of the functional additives in the substrate.

Table 3
UV transmittance rate of nanocomposites

Wavelength (nm)		PLA	NS	NCC	PS1	PS3	PS5	PS7	PS9	PC1	PC3
254	AT rate (%)	83.1	61.6	53.2	71.6	63.1	16.9	35.2	34.3	61.7	55.2
	SD	0.1	0.2	0.2	0.7	0.8	0.5	1.2	0.6	4.6	3.4
277	AT rate (%)	80.9	62.7	59.8	56.7	51.1	15.8	28.9	28.4	50.0	44.0
	SD	0.4	0.2	0.1	0.5	1.2	0.3	0.9	0.4	3.9	0.7
300	AT rate (%)	83.9	62.8	65.3	80.7	72.6	24.4	43.7	42.7	70.5	63.7
	SD	0.2	0.3	0.2	0.9	0.8	1.2	1.3	0.5	1.7	0.7
400	AT rate (%)	83.9	66.4	75.0	81.0	72.8	45.8	43.7	42.8	70.0	63.8
	SD	0.1	0.2	0.1	0.7	0.5	1.1	1.3	0.5	1.7	0.9

Wavelength (nm)		PC5	PC7	PC9	PS3C1	PS3C3	PS3C5	PS3C7	PS3C9
254	AT rate (%)	50.7	34.8	27.2	42.4	57.8	25.3	15.6	29.9
	SD	0.8	0.5	1.0	0.4	0.6	1.0	1.5	1.1
277	AT rate (%)	41.7	27.8	22.1	34.7	46.9	19.5	11.8	23.2
	SD	0.7	0.5	0.9	0.1	0.8	0.8	1.1	1.1
300	AT rate (%)	53.2	36.9	29.0	49.7	60.4	26.0	19.1	30.3
	SD	1.0	1.1	0.7	0.5	0.3	0.8	0.7	0.2
400	ATR (%)	53.5	37.0	28.7	53.7	64.9	27.5	20.2	32.1
	SD	0.8	1.0	1.1	0.2	0.4	0.5	1.4	0.5

ATR: average UV transmittance rate
SD: standard deviation

CONCLUSION

Adding suitable quantities of NS and/or NCC to a PLA substrate could improve the overall thermal stability, mechanical strength and UV shielding capacity of the resulting nanocomposites. Simultaneous addition of NS and NCC to the composite substrate exerted a greater contribution to the enhancement of the overall functionalities than did those with bipartite components. The shortcoming of weak bonding between NS and PLA could be ameliorated with the addition of NCC. Based on our results, at a 3% NS and 7% NCC addition rate to the PLA substrate, the most optimal tensile strength was obtained. At temperatures <250 °C, the nanocomposites exhibited good thermal stability, and could effectively block about 65% of UVB and UVC irradiation. In the future, the

formulations might be applied as a biodegradable UV shielding coating film; or be applied alone as a medical wrapping material or packaging material.

ACKNOWLEDGMENTS: The Sunshine Mineral Co. Ltd. Taitung, Taiwan, kindly provided the sericite. Ms. Irene Chen and the staff of the Division of Wood Cellulose, Taiwan Forestry Research Institute provided irreplaceable assistance and instrumental helps. We hereby acknowledge their contributions.

REFERENCES

[1] D. E. Henton, P. Gruber, J. Lunt and J. Randall, in "Natural Fibers, Biopolymers, and Biocomposites", edited by A. K. Mohanty, M. Misra, L. T. Drzal, Florida, Taylor & Francis Group, 2005, pp. 538-547.
[2] F. Ikazaki, K. Uchida, K. Kamiya, A. Kawai, A. Gotoh and E. Akiba, *Int. J. Miner. Process*, **44-45**, 93 (1996).
[3] H. A. Essawy, A. Nourelhoda, E. W. Abd, A. Mahmoud and E. G. Abd, *Polym. Degrad. Stabil.*, **93**, 1472 (2008).
[4] L. Hai, W. G. Kang, M. Huang, D. Ding and X. Xu, *J. Univ. Sci. Technol.*, **B 25**, 627 (2004), [in Chinese with English summary].
[5] H. Uno, K. Tamura, H. Yamada, K. Umeyama, T. Hatta and Y. Moriyoshi, *Appl. Clay Sci.*, **46**, 81 (2009).
[6] L. Petersson and K. Oksman, *Compos. Sci. Technol.*, **66**, 2187 (2006).
[7] S. S. Ray and M. Bousmina, *Prog. Mater. Sci.*, **50**, 962 (2005).
[8] D. Bondeson, A. Mathew and K. Oksman, *Cellulose*, **13**, 171 (2006).
[9] M. A. Hubbe, O. J. Rojas, L. A. Lucia and M. Sain, *BioResources*, **3**, 929 (2008).
[10] N. Ljungberg, C. Bonini, F. Bortolussi, C. Boisson, L. Heux and J. Y. Cavaillé, *Biomacromolecules*, **6**, 2732 (2005).
[11] N. L. G. Rodriguez, W. Thielemans and A. Dufresne, *Cellulose*, **13**, 261 (2006).
[12] M. D. Sanchez–Garcia, E. Gimenez and J. M. Lagaron, *Carbohyd. Polym.*, **71**, 235 (2008).
[13] J. Summerscales, P. J. N. Dissanayake, S.V. Amandeep and H. Wayne, *Composites A*, **41**, 1329 (2010).
[14] J. Summerscales, P. J. N. Dissanayake, S.V. Amandeep and H. Wayne, *Composites A*, **41**, 1336 (2010).
[15] N. Nosbi, H. M. Akil, Z. A. M. Ishak and A. A. Bakar, *Mater. Des.*, **31**, 4960 (2010).
[16] C. W. China and B. F. Yousifb, *Wear*, **267**, 1550 (2009).
[17] B. H. Lee, H. S. Kim, S. Lee, H. J. Kim and J. R. Dorgan, *Compos. Sci. Technol.*, **69**, 2573 (2009).
[18] C. P. Chang, I. C. Wang, K. J. Hung and Y. S. Perng, *Taiwan. J. For. Sci.*, **25**, 231 (2010).
[19] K. Das, D. Ray, N. R. Bandyopadhyay, T. Ghosh, A. K. Mohanty and M. Misra, *Cellulose*, **16**, 783 (2009).
[20] D. G. Gray, *Cellulose*, **15**, 297 (2008).
[21] A. Pei, Q. Zhou and L. A. Berglundm, *Compos. Sci. Technol.*, **70**, 815 (2010).